

# Investigation of nonlinear-absorption anisotropy in YAG:Cr<sup>4+</sup>

N. N. Il'ichev, A. V. Kir'yanov, P. P. Pashinin, and S. M. Shpuga

*Institute of General Physics, Russian Academy of Sciences, 117942 Moscow, Russia*

(Submitted 1 December 1993)

*Zh. Eksp. Teor. Fiz.* **105**, 1426–1441 (May 1994)

The polarization characteristics of nonlinear absorption in a YAG:Cr<sup>4+</sup> crystal at saturation under resonant excitation at 1.06  $\mu\text{m}$  were investigated in the case when the duration of the pulse propagating in the crystal is significantly shorter than the lifetime of the excited state of the Cr<sup>4+</sup> impurity centers. The experimental data are described by a phenomenological model in which resonant absorption in the crystal is characterized by three linear dipoles oriented along the crystallographic axes of the YAG. The theoretical calculations are in good agreement with the experimental data.

## 1. INTRODUCTION

Garnet-based crystals (GSGG, GSAG, and YAG) with chromium impurity ions are of great interest as promising laser materials in the visible and near IR. Attention has been focused on crystals with so-called phototropic Cr<sup>4+</sup> impurity centers.<sup>1–4</sup> These crystals are of interest if only because the nature of these centers has yet to be determined. Most authors now agree that these centers are chromium ions with valence 4, which in the garnet-based crystals replace Al<sup>3+</sup> or Ga<sup>3+</sup> ions and participate in tetrahedral and octahedral coordinations of O<sup>2-</sup> oxygen ligands.<sup>4–6</sup> It is believed that the Cr<sub>tetr</sub><sup>4+</sup> impurity centers are responsible for absorption by the crystal in the 8000–13 000 cm<sup>-1</sup> bands and luminescence in the 6000–9000 cm<sup>-1</sup> range, while the Cr<sub>oct</sub><sup>4+</sup> centers are responsible for absorption in the 15 000–30 000 cm<sup>-1</sup> range and do not luminesce.<sup>6,7</sup>

This concept must be treated with caution, however, since chromium ions with valence 4 have yet to be observed in nature<sup>8</sup> (information about the possibility of Cr<sup>4+</sup> ions in the lattice of the mineral forsterite—Mg<sub>2</sub>SiO<sub>4</sub>:Cr<sup>4+</sup>—has appeared only recently<sup>9</sup>). Moreover, as pointed out in Ref. 5 and 8, Cr<sup>4+</sup> ions can appear in garnet-based crystals only if Mg or Ca impurities are added to chromium to the melt from which the crystals are grown and the appropriate heat treatment is carried out. No definite dependence of the Cr<sub>tetr</sub><sup>4+</sup> concentration on the chromium concentration in the melt is observed. For this reason, the Cr<sup>4+</sup> centers being color centers similar to those in a number of alkali-halide crystals, for example, has not been ruled out. The Cr ions can then have their usual valence 3, and the specific properties of the impurity garnets which are under discussion could be determined by various unidentified defects.

The foregoing information concerning the nature of Cr<sup>4+</sup> impurity centers in garnets demonstrates the timeliness of investigating such media carefully. On the other hand, the progress made in applications of these crystals (GSGG:Cr<sup>4+</sup>, GSAG:Cr<sup>4+</sup>, and YAG:Cr<sup>4+</sup>) to the physics of visible and near-IR lasers should be underscored. Thus, passive mode-locking<sup>10</sup> and passive Q-switching<sup>11,12</sup> of neodymium lasers operating at  $\lambda \sim 1.06 \mu\text{m}$  have been

achieved with the help of these crystals. This was made possible by the fact that the Cr<sup>4+</sup> centers have two effective lifetimes in the excited state:  $T_{(1)} \sim 500$  psec (Ref. 10) and  $T_{(2)} \sim 2\text{--}4 \mu\text{sec}$ .<sup>10,13</sup> The possibility of developing efficient lasers with a YAG:Cr<sup>4+</sup> active element, which are tunable over the wavelength range 1.4–1.6  $\mu\text{m}$  (the luminescence range of Cr<sub>tetr</sub><sup>4+</sup> centers), has been demonstrated in Refs. 14 and 15 with laser pumping at  $\lambda \sim 1.06 \mu\text{m}$ .

In the present paper we examine the nonlinear effects that appear at the absorption-saturation stage and are caused by bleaching of the phototropic Cr<sup>4+</sup> impurity centers in a YAG crystal during the propagation of a short (pulse duration  $\tau_p \ll T_{(2)}$ ) resonant light pulse ( $\lambda \sim 1.06 \mu\text{m}$ ). As shown in Ref. 16 for a similar problem in LiF alkali-halide crystals with F<sub>2</sub><sup>-</sup> color centers, when radiation propagates in a doped crystal, polarization and orientational absorption anisotropy appear at the saturation stage. Self-induced rotation of the polarization plane of the wave propagating in the crystal also appears.<sup>16,17</sup> Since LiF:F<sub>2</sub><sup>-</sup> and YAG:Cr<sup>4+</sup> crystals are similar from the standpoint of models, i.e., they are variants of a nonrandom distribution of the possible orientations of resonantly absorbing dipoles relative to the crystal lattice, it is of interest to compare the manifestations of these effects in these two media. Moreover, information about the properties of Cr<sup>4+</sup> centers observed in experiments of the type performed in Ref. 16 can be used to develop a faithful model of these centers in garnets, the need for which was demonstrated above.

Absorption anisotropy at the saturation stage in YAG:Cr<sup>4+</sup> was observed experimentally in Ref. 18. There, however, the change in the polarization state of radiation traversing the crystal was not studied, and no theoretical description of the indicated phenomena was given. The present paper fills in these gaps.

## 2. EXPERIMENTAL APPARATUS AND MEASUREMENT PROCEDURE

### Description of apparatus

The pulses ( $\tau_p \sim 100$  nsec) generated by Q-switched neodymium lasers satisfy the condition  $\tau_p \ll T_{(2)}$ . In this connection, just as in Ref. 17, a neodymium phosphate

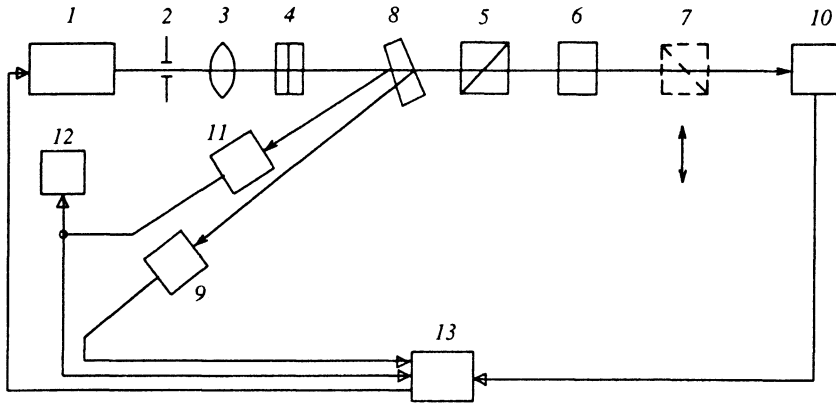


FIG. 1. Experimental arrangement: 1—laser, 2—diaphragm, 3—lens, 4—attenuating filters, 5, 7—Glan prisms, 6—experimental crystal, 8—beamsplitter (wedge), 9, 10—photodiode detectors, 11—trigger photodiode, 12—oscillograph, 13—personal computer.

glass laser operating in the single-frequency regime in transverse  $TEM_{00}$  mode (beam diameter 1.5 mm) was used in the experiment. The laser resonator was  $Q$ -switched with a  $LiF:F_2^-$  crystal.<sup>19</sup> The pulse energy was  $\sim 2$  mJ, the laser pulse duration was  $\sim 25$  nsec, and the pulse repetition frequency was 1–2 Hz.

As follows from Fig. 1, an image of a diaphragm 2, separating a beam with a nearly rectangular distribution, is constructed with the help of a lens 3 at the center of the  $YAG:Cr^{4+}$  crystal 6. Neutral-density filters 4 attenuate the beam, and the polarizer 5 produces highly polarized radiation ( $\sim 1/4000$ ). The beam energy at the entrance and exit of the crystal can be measured with the beamsplitter 8 and photodiodes 9 and 10, whose load consists of integrating circuits with  $\tau_{int} \sim 10$  msec. Photodiode 11 triggers the automatic measuring system. Electrical signals from photodiodes 9 and 10 are processed by the computer 12. A detailed description of the experimental apparatus is given in Ref. 16.

In the course of the experiment the transmission coefficient  $T$  of the crystal and the self-induced rotation  $\Delta\theta$  of the polarization plane of the wave at the exit of the crystal were measured as a function of the position  $\theta_0$  of the polarization plane at the crystal entrance.

### Measurement procedure

To measure the function  $T(\theta_0)$ , a  $YAG:Cr^{4+}$  sample mounted in a frame was rotated about the optical axis of the apparatus. To avoid undesirable interference effects due to reflection from the faces, the crystal was turned with respect to the optical axis by a small angle ( $\sim 1-2^\circ$ ). The sample was placed in the rotating frame in a manner so as to ensure minimum beam displacement in the crystal aperture as the crystal rotated. The function  $T(\theta_0)$  was determined by measuring the energies  $E_1$  and  $E_2$  recorded with photodiodes 9 and 10. Here  $T = E_2/E_1$ .

The optical arrangement was altered to measure  $\Delta\theta(\theta_0)$ . Specifically, an analyzer 7, similar to the polarizer, was installed at the exit of the  $YAG:Cr^{4+}$  sample. The energy  $E_2$  as a function of the angle  $\beta$ , which characterizes the deviation from the position of completely crossed analyzer and polarizer (see Fig. 2), was measured for each value of  $\theta_0$ . The angle  $\beta$  was varied near the minimum of the transmission function  $E_2(\beta)$  of the polarizer-crystal-

analyzer system. The value of  $\beta_0$  corresponding to the minimum of this function was calculated by fitting  $E_2(\beta)$  with a parabolic function. The quantity  $\beta_0 = \Delta\theta$  [see Eq. (A9) in the Appendix], i.e., it is the desired angle of self-induced rotation of the polarization plane of the wave. Thus the required function can be obtained by calculating the value of  $\beta_0$  for each value of  $\theta_0$ .

The energy  $E_1$  of the wave incident on the crystal is a parameter in the functions  $T(\theta_0)$  and  $\Delta\theta(\theta_0)$ . A family of these functions can be obtained by varying the attenuation of the beam using the neutral-density filters 4.

### Object of Investigation

The experimental  $YAG:Cr^{4+}$  crystal was a cylindrical plate 9.45 mm in diameter with a 4.65 mm generatrix. The crystal faces were AR coated (at  $\lambda \sim 1 \mu m$ ). Radiation

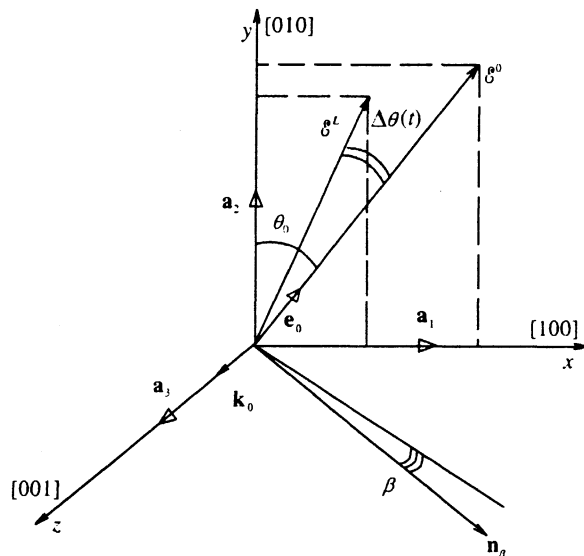


FIG. 2. Schematic diagram of the interaction of the resonance radiation ( $\lambda \sim 1.06 \mu m$ ) with a  $YAG:Cr^{4+}$  crystal.  $x, y, z$ —directions of the crystallographic axes of YAG. The vectors  $a_i$  indicate the position of the three groups of linear dipoles or three groups of circular dipoles characterizing the  $Cr^{4+}$  impurity in YAG. The angle  $\theta_0$  fixes the position of the polarization plane of the radiation at the entrance of the crystal. The angle  $\beta$  fixes the position of minimum transmission of the polarizer at the exit of the crystal. The angle  $\Delta\theta(t)$  is the rotation angle of the polarization at the exit from  $YAG:Cr^{4+}$ .

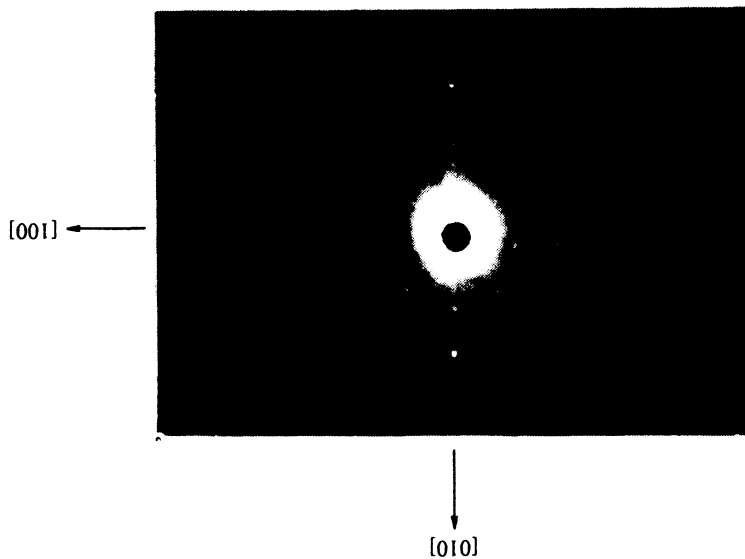


FIG. 3. Laue pattern of the YAG:Cr<sup>4+</sup> sample. The crystallographic axes correspond to Fig. 2 (the brightest cross in the photograph).

incident in the normal direction on a crystal face propagated along one of the crystallographic axes of the YAG. Figure 3 displays the Laue pattern of the experimental sample. The arrows mark the directions of the two other crystallographic axes, which lie in the plane of the crystal faces (the brightest cross in the photograph). It should be noted that in Fig. 2 the axes of the coordinate system ( $x, y, z$ ) chosen for the calculation (see Sec. 4) are oriented along the [100], [010], and [001] crystallographic axes of the YAG (compare to Fig. 3).

### 3. EXPERIMENTAL RESULTS AND DISCUSSION

The transmission coefficient of a YAG:Cr<sup>4+</sup> crystal was determined first with a weak signal, for which  $T_0 \approx 24.5\%$  independent of the position  $\theta_0$  of the polarization plane of the wave at the entrance of the crystal. The polarization state of the radiation at the exit from the crystal did not change. As expected, with respect to weak probe radiation, the YAG:Cr<sup>4+</sup> crystal behaved as an optically isotropic medium.

As the energy  $E_1$  of the incident pulse increased, the transmission coefficient of YAG:Cr<sup>4+</sup> increased, approaching  $T_f \approx 80\%$  in the completely bleached state of the crystal. Figure 4 displays a family of curves  $T(\theta_0)$  (a) and  $\Delta\theta(\theta_0)$  (b). Curves 1–3 in both figures correspond to different values of the incident energy  $E_1$ . The period as a

function of  $\theta_0$  is clearly  $90^\circ$ , the maxima  $T_{\max}$  of the transmission coefficient correspond to  $\theta_0 = 0^\circ, \pm 90^\circ, \dots$  and the minima  $T_{\min}$  correspond to  $\theta_0 = \pm 45^\circ, \pm 135^\circ, \dots$  (Fig. 4a). As  $E_1$  increases, the transmission contrast

$$D = (T_{\max} - T_{\min}) / \bar{T},$$

where  $\bar{T} = (T_{\max} + T_{\min}) / 2$  is the average transmission coefficient of the crystal, first increases to the maximum value, corresponding to  $\bar{T} \approx 45\%$ , and then decreases, approaching zero as  $\bar{T} \rightarrow T_f$ .

From Fig. 4b, the maximum rotation angle  $\Delta\theta_{\max} \approx 5.5^\circ$  is reached at  $\bar{T} \approx 57\%$ . Comparing the plots in Figs. 4a and b we find that the extrema of the transmission function  $T(\theta_0)$  correspond to the zeros of the function  $\Delta\theta(\theta_0)$ —for any incident energy, radiation propagates in the crystal without a change in polarization state only for these values of  $\theta_0$ .

Another interesting property is the decrease in the widths of the maxima of the function  $T(\theta_0)$  with increasing energy incident pulse. In the limit  $E_1 \rightarrow \infty$  ( $T \rightarrow T_f$ ), as will be shown below (see Sec. 4), their width must approach zero.

Figure 5a displays the nonlinear-transmission contrast  $D$  versus the average transmission  $\bar{T}$  of the crystal. Figure 5b displays the change  $\Delta\theta_{\max}$  in the maximum rotation angle of the polarization plane of the wave at the exit from

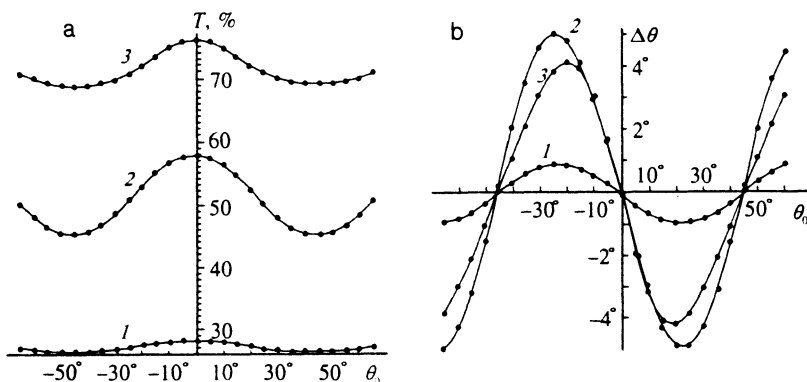


FIG. 4. (a) Experimental curves of the transmission coefficient  $T$  of a YAG:Cr<sup>4+</sup> crystal, and (b) the rotation angle  $\Delta\theta$  of the polarization plane at the exit of the crystal as functions of the position  $\theta_0$  of the polarization plane of the wave at the entrance to the crystal. The curves were constructed for three different values of the incident radiation energy density corresponding to transmission  $T \approx 27\%$  (1),  $\approx 50\%$  (2), and  $\approx 72\%$  (3).

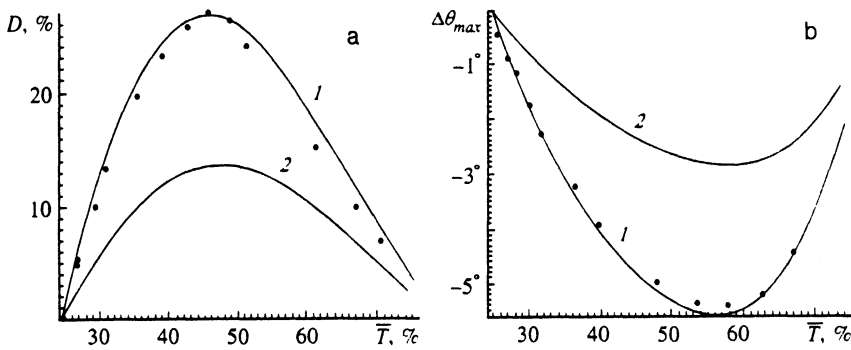


FIG. 5. (a) Transmission contrast  $D$ , and (b) maximum rotation angle  $\Delta\theta_{\max}$  of the polarization plane as functions of the average transmission  $\bar{T}$  of the YAG:Cr<sup>4+</sup> crystal. Dots—experiment; curves: 1—theory, model of three linear dipoles; 2—theory, model of three circular dipoles.

the crystal as a function of  $\bar{T}$ . The value  $\bar{T} \approx 75\%$  corresponds to the maximum possible energy  $E_1$  of the incident radiation in this experiment (this value of the transmission is reached without the attenuating filters in front of the crystal, the energy density of the wave at the location of the crystal being  $\sim 1 \text{ J/cm}^2$ ).

The experimental curves in Figs. 4 and 5 make it possible to construct a phenomenological model of the interaction of a short resonant radiation pulse with a YAG:Cr<sup>4+</sup> crystal. First, we must make a number of remarks.

1. The existence of induced anisotropy of the transmission coefficient and the presence of the corresponding self-induced rotation of the polarization plane of the wave indicate that the resonantly absorbing dipoles, which characterize the additional absorption of the crystal at  $\lambda \sim 1.06 \mu\text{m}$ , are not randomly oriented with respect to the crystal lattice of the YAG. In other words, there exist groups of these dipoles with definite directions of orientation (see Refs. 20 and 21).

2. It is obvious from symmetry considerations that in a cubic crystal, resonant dipoles can be oriented along one of  $12/n$  possible  $n$ -fold axes ( $n=4, 3, 2$ ) (see, for example, Ref. 22), i.e., on the basis of the remarks made above, the resonant dipoles characterizing the absorption of Cr<sup>4+</sup> impurity centers at  $\lambda \sim 1.06 \mu\text{m}$  can assume three, four, or six orientations.

3. As one can see from Fig. 4, no additional maxima of the transmission function  $T(\theta_0)$  and no additional zeros of the function  $\Delta\theta(\theta_0)$  appear as the energy of the incident radiation increases. It is well known<sup>17</sup> that additional maxima appear in the case of an LiF:F<sub>2</sub><sup>-</sup> crystal, in which the resonantly absorbing dipoles (F<sub>2</sub><sup>-</sup> color centers) can take on six orientations.<sup>23</sup> Thus, on the basis of what we have said above, the dipoles characterizing the Cr<sup>4+</sup> impurity centers can take on either three or four orientations.

4. In accordance with Fig. 4, the maxima of the transmission function of YAG:Cr<sup>4+</sup> occur for directions  $\theta_0$  of the electric vector of the wave that correspond to the crystallographic axes of the YAG crystal (Fig. 3). Taking into consideration the method by which the angles  $\theta_0$  were measured in the experiment (see Fig. 2), we arrive at the unequivocal conclusion that the YAG crystal contains three groups of resonant dipoles, characterizing absorption at  $\lambda \sim 1.06 \mu\text{m}$  and oriented along the [100], [010], and [001] crystallographic axes of the crystal.

There remains the question of which type of dipoles characterize the Cr<sup>4+</sup> impurity in a YAG crystal with resonant interaction at  $1.06 \mu\text{m}$ —circular, as assumed, for example, in Ref. 13, or linear, as proposed in Ref. 18. The answer to this question can be obtained only by comparing the experimental data to a theoretical model of the interaction process.

#### 4. THEORY

Let a linearly polarized plane wave with electric vector  $\mathcal{E}(x, y, z, t)$  propagate in a YAG:Cr<sup>4+</sup> crystal. Assuming that the amplitude  $\mathcal{E}^0(x, y, z, t)$  of the wave  $\mathcal{E} = \mathcal{E}^0 \exp[i(k_0 z - \omega t)]$  varies slowly, the following equation can be derived from Maxwell's equations for the field in a resonant medium (see, for example, Ref. 20):

$$\frac{\partial \mathcal{E}^0}{\partial z} + \frac{\sqrt{\epsilon'}}{c} \frac{\partial \mathcal{E}^0}{\partial t} + \frac{\mathcal{E}^0 \gamma}{2} = \frac{2\pi i \omega}{c \sqrt{\epsilon'}} \mathcal{P}^0, \quad (1)$$

where  $\mathcal{P}^0(x, y, z, t)$  is the slowly varying amplitude of the polarization of the resonant transition  $\mathcal{P}^0 = \mathcal{P} \exp[-i(k_0 z - \omega t)]$ ,  $\epsilon = \epsilon' + j\epsilon''$  is the dielectric constant of the medium neglecting the resonant transition,  $\omega$  and  $k_0 = \omega \sqrt{\epsilon'}/c$  are, respectively, the frequency and wave vector of the wave, and  $\gamma = k_0 \epsilon''/\epsilon'$  is the coefficient of linear (nonresonant) losses. The equation (1) is valid if  $|\partial \mathcal{E}^0/\partial z| \ll k_0 \mathcal{E}^0$ , and  $|\partial \mathcal{E}^0/\partial t| \ll \omega \mathcal{E}^0$ .

We have for the polarization amplitude  $\mathcal{P}^0$

$$\mathcal{P}^0 = \tilde{\kappa} \sum_{i=1}^3 N_i \mathbf{a}_i(\mathcal{E}^0, \mathbf{a}_i), \quad (2)$$

where  $\mathbf{a}_i$  are unit vectors of the dipoles that characterize the resonance transition in YAG:Cr<sup>4+</sup>, and  $\tilde{\kappa}$  is the complex polarizability of an individual dipole. For definiteness, the dipoles are assumed to be linear. The summation in Eq. (2) is performed, in accordance with the results of Sec. 3, for  $i=1, 2$ , and 3.

Since  $\tilde{\kappa} \equiv \kappa' + i\kappa''$  and from general considerations  $\kappa' = \delta\kappa''$ , where  $\delta$  is a proportionality factor, the following relation can be written down between the imaginary part  $\kappa''$  of the susceptibility and the absorption coefficient  $\alpha_0$  of the crystal in the unbleached state:

$$\alpha_0 = \frac{4\pi\omega\kappa'' N_0}{3c\sqrt{\epsilon'}} \quad (3)$$

and the quantity

$$\tilde{\alpha}_0 = \alpha_0(1 - i\delta) \quad (4)$$

establishes the relation between the real and imaginary parts of the susceptibility  $\tilde{\kappa}$ . In (3),  $N_0$  is the concentration of  $\text{Cr}^{4+}$  impurity centers in the YAG crystal and  $N_0/3$  is the concentration of these centers with  $i$ th orientation in the unexcited crystal in the lower level.

In projections on the axes chosen in accordance with Fig. 2, Eq. (1) can be written, using (2)–(4), as

$$\frac{\partial \mathcal{E}_i^0}{\partial z} + \frac{\sqrt{\varepsilon'}}{c} \frac{\partial \mathcal{E}_i^0}{\partial t} + \frac{\mathcal{E}_i^0 \gamma}{2} = -\frac{\tilde{\alpha}_0}{2} \frac{3}{N_0} N_i \mathcal{E}_i^0, \quad (5)$$

where  $\mathcal{E}_i^0 (i=x, y)$  are the projections of the vector  $\mathcal{E}^0$  on the  $x$  or  $y$  axis, and  $N_i (i=x, y)$  are the concentrations of the dipoles with the corresponding orientation in the lower level.

Next, since  $\mathcal{E}^0$  is a complex quantity ( $\mathcal{E}_i^0 = \mathcal{E}_i \exp(i\varphi_i)$ ), we obtain the following equations for the components of the real amplitude  $\mathcal{E}_i$  and the phase  $\varphi_i$ :

$$\frac{\partial \mathcal{E}_i}{\partial z} + \frac{\sqrt{\varepsilon'}}{c} \frac{\partial \mathcal{E}_i}{\partial t} = -\frac{\mathcal{E}_i}{2} \left( \gamma + \alpha_0 \frac{3N_i}{N_0} \right), \quad (6)$$

$$\frac{\partial \varphi_i}{\partial z} + \frac{\sqrt{\varepsilon'}}{c} \frac{\partial \varphi_i}{\partial t} = \frac{\alpha \delta_0}{2} \frac{3N_i}{N_0}. \quad (7)$$

The concentration of dipoles with the  $i$ th orientation in the ground state is time-dependent,  $N_i = N_i(t)$ . Obviously  $N_i(0) = N_0/3$ . Setting

$$n_i = \frac{N_i(t)}{N_i(0)} = \frac{3N_i}{N_0}, \quad (8)$$

we can therefore write for the total differential  $dn_i/dt$

$$\frac{dn_i}{dt} = -\sigma_0 n_i I_i \quad (9)$$

since  $\tau_p \ll T_{(2)}$ . Here  $I_i$  are the intensities of the  $x$  and  $y$  components of the wave propagating in the crystal. In Eq. (9), in accordance with the proposed dipole character of the interaction of the wave with  $\text{Cr}^{4+}$  center, the quantity  $\sigma_0$  is the maximum absorption cross section (when  $\mathcal{E}^0 \parallel \mathbf{a}_i$ ), with

$$\sigma_i = \sigma_0 (\mathbf{e}_0, \mathbf{a}_i)^2 \quad (10)$$

and  $\mathbf{e}_0$  (see Fig. 2) is a unit vector in the direction of the electric vector  $\mathcal{E}^0$  of the wave,  $\mathcal{E}^0 = \mathbf{e}_0 \mathcal{E}^0$ .

Taking Eqs. (8)–(10) into consideration, we obtain from (6)–(7) the following system of equations for  $I_i$ :

$$\frac{\partial I_i}{\partial z} + \frac{\sqrt{\varepsilon'}}{c} \frac{\partial I_i}{\partial t} = -\alpha_0 n_i I_i - \gamma I_i,$$

$$\frac{\partial \varphi_i}{\partial z} + \frac{\sqrt{\varepsilon'}}{c} \frac{\partial \varphi_i}{\partial t} = -\frac{\delta}{2} \alpha_0 n_i, \quad (11)$$

$$\frac{dn_i}{dt} = -\sigma_0 n_i I_i.$$

In what follows we shall be interested only in the final (post-interaction) states of the wave and the YAG:Cr<sup>4+</sup> crystal. Accordingly, we define the parameter

$$A(z) = \sigma_0 \int_{-\infty}^{\infty} I(z, t) dt, \quad (12)$$

which characterizes the energy density of the light pulse. The energy densities of the pulses propagating in the  $x$  or  $y$  direction can be determined completely analogously:

$$A_i(z) = \sigma_0 \int_{-\infty}^{\infty} I_i(z, t) dt, \quad (13)$$

with  $A_x + A_y = A$ .

It is shown in Ref. 16 that for a short light pulse ( $\tau_p \ll T_{(2)}$ ) the rotation of the polarization plane in an impurity crystal can be characterized by the quantity

$$\Delta\theta(z) = \frac{\int_{-\infty}^{\infty} \Delta\theta(z, t) I(z, t) dt}{\int_{-\infty}^{\infty} I(z, t) dt}, \quad (14)$$

i.e., by the average rotation angle over the pulse interaction time.

Next, by analogy, we define the ‘‘pulse average’’ phase runout  $\Delta\varphi = |\varphi_x - \varphi_y|$  between the  $x$  and  $y$  components of the wave to be

$$\Delta\varphi(z) = \frac{\int_{-\infty}^{\infty} \Delta\varphi(t) I(z, t) dt}{\int_{-\infty}^{\infty} I(z, t) dt}. \quad (15)$$

Likewise, we take

$$B \equiv A\Delta\theta(z), \quad C \equiv A\Delta\varphi(z). \quad (16)$$

The system of equations (11) together with the definitions (12)–(16) completely describe the solution of the problem of a short light pulse traversing a YAG:Cr<sup>4+</sup> crystal in the dipole approximation of the interaction.

The solution of the system (11) makes it possible to compare the theoretical results with the experimental data. In the course of the experiment, the nonlinear-transmission coefficient  $T$  of the YAG:Cr<sup>4+</sup> crystal was measured as the ratio of the energies of the transmitted and incident radiation, i.e.,  $T = A_{z=L}/A_{z=0}$ , where  $L$  is the length of the crystal. The pulse-averaged phase shift of the wave and the rotation of the major axis of the polarization ellipse after traversing the crystal are given by  $\Delta\varphi = C_{z=L}/A_{z=L}$  and  $\Delta\theta = B_{z=L}/A_{z=L}$ , respectively.

Figure 6 displays  $T$ ,  $\Delta\theta$ , and  $\Delta\varphi$  as functions of the position  $\theta_0$  of the polarization plane of the radiation at the entrance into the crystal. They were obtained by numerically integrating the system of equations (11) by the Runge–Kutta method for a YAG:Cr<sup>4+</sup> crystal of length  $L = 0.5$  cm with initial transmission  $T_0 = 24.5\%$  and final transmission  $T_f = 80.0\%$ . The values of  $L$ ,  $T_0$ , and  $T_f$  were chosen in accordance with the characteristics of the experimental sample (see Sec. 3). The calculation was performed for  $A_{z=0} = 7.5$ , which corresponds to the average transmission of the crystal  $\bar{T} \approx 60\%$ . Figure 6 also displays the experimental curves of  $T$  and  $\Delta\theta$  versus the angle  $\theta_0$  (similar to those shown in Fig. 4) as well as  $\Delta\varphi(\theta_0)$  (see Sec. 5).

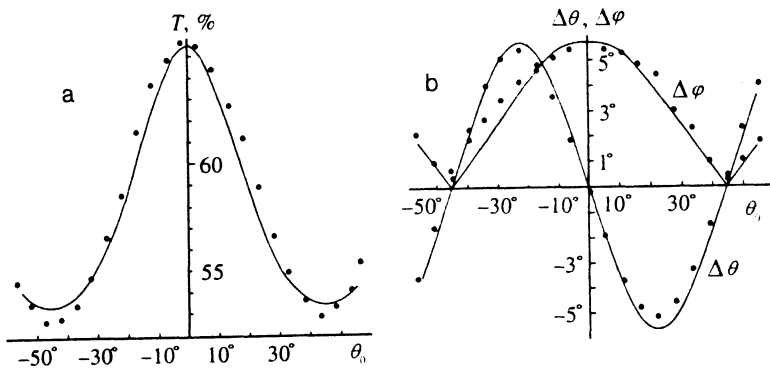


FIG. 6. (a) Transmission coefficient  $T$  of a YAG:Cr<sup>4+</sup> crystal and (b) difference between the phase increments  $\Delta\varphi$  of the  $x$  and  $y$  components of the wave and the rotation angle  $\Delta\theta$  of the major axis of the polarization ellipse versus the position  $\theta_0$  of the polarization plane of the wave at the entrance to the crystal. Dots—experiment; solid lines—theory (model of three linear dipoles). The average transmission of the crystal is  $\bar{T} \approx 60\%$ .

The computational results obtained for the system (11) for different values of the incident energy density incident on the crystal (i.e., different values of  $A_{z=0}$ ) are presented in Fig. 5 together with the experimental data (curves 1)—the theoretical curves of the transmission contrast  $D$  and the angle  $\Delta\theta_{\max}$  as a function of the average transmission  $\bar{T}$  in the model of three linear dipoles are displayed.

We now present a system of equations that describes the interaction of resonant radiation with a system of three circular dipoles. A number of authors have taken up the model of three orthogonal circular dipoles (see, for example, Ref. 13) to describe the interaction of radiation with a YAG:Cr<sup>4+</sup> crystal at  $\lambda \sim 1 \mu\text{m}$ . By a circular dipole oriented, for example, along the  $X$  axis we mean a dipole absorbing radiation whose electric field vector lies in the  $(y,z)$  plane. Circular dipoles for the other two types of possible orientations are defined similarly. It is easy to show that the system of equations describing the interaction in this case has the form

$$\begin{aligned} \frac{\partial I_x}{\partial z} + \frac{\sqrt{\epsilon'}}{c} \frac{\partial I_x}{\partial t} &= -\left(\gamma + \frac{\alpha_0}{2} n_y - \frac{\alpha_0}{2} n_z\right) I_x, \\ \frac{\partial I_y}{\partial z} + \frac{\sqrt{\epsilon'}}{c} \frac{\partial I_y}{\partial t} &= -\left(\gamma + \frac{\alpha_0}{2} n_x - \frac{\alpha_0}{2} n_z\right) I_y, \\ \frac{dn_x}{dt} &= -\sigma_0 n_x I_y, \\ \frac{dn_y}{dt} &= -\sigma_0 n_y I_x, \\ \frac{dn_z}{dt} &= -\sigma_0 n_z (I_x + I_y). \end{aligned} \quad (17)$$

Solving the system of equations numerically we can obtain, in particular, the functions presented in Fig. 5 (curves 2).

Comparing the experimental and theoretical curves shown in Fig. 5 (constructed for both models), we arrive at the following basic conclusion. The experimental results are described best by the phenomenological model of phototropic Cr<sup>4+</sup> impurity centers in YAG as three linear dipoles, oriented along the crystallographic axes of YAG and absorbing resonantly at a wavelength of  $\lambda \sim 1.06 \mu\text{m}$ . The model of three circular dipoles, presupposing that the

Cr<sup>4+</sup> ions are described as ions (not color centers) in a distorted tetrahedral environment of oxygen ligands, is not consistent with the experimental data. This conclusion is drawn on the basis of the fact that the experimental data agree quantitatively with the computational results obtained with the model of three linear dipoles (11) for all parameters investigated ( $T, \Delta\theta, \Delta\varphi$ ).

At the same time, the model in which, for a different section of the spectrum of resonant absorption of a YAG:Cr<sup>4+</sup> crystal in the near IR (extending from 0.8 to 1.2  $\mu\text{m}$ ), the Cr<sup>4+</sup> impurity can also be described by a model of three circular dipoles, has not been ruled out (just as, by the way, the intermediate case between the models of three linear and three circular dipoles can also be observed). However, this question is not considered here.

In conclusion we turn to Fig. 7, which displays the theoretical curves (for both models) of the width  $\Psi$  of the maxima of the transmission function  $T(\theta_0)$  versus the average transmission  $\bar{T}$ . The figure also shows the experimental values of  $\Psi(\bar{T})$  obtained by analyzing the functions  $T = T(\theta_0)$  (see Figs. 4 and 6). Better agreement between the theoretical and experimental curves is observed, as is evident from Fig. 7, for the model of three linear dipoles.

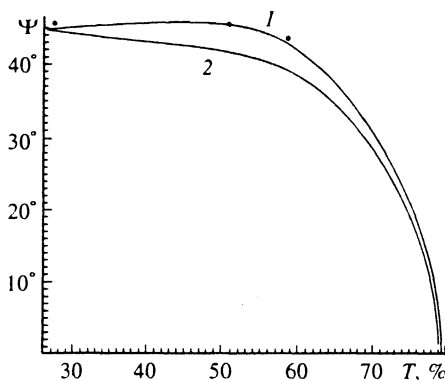


FIG. 7. Width  $\Psi$  of the maxima of the transmission function  $T(\theta_0)$  versus the average transmission coefficient  $\bar{T}$ . Dots—experiment; curves: 1—theory, model of three linear dipoles; 2—theory, model of three circular dipoles.

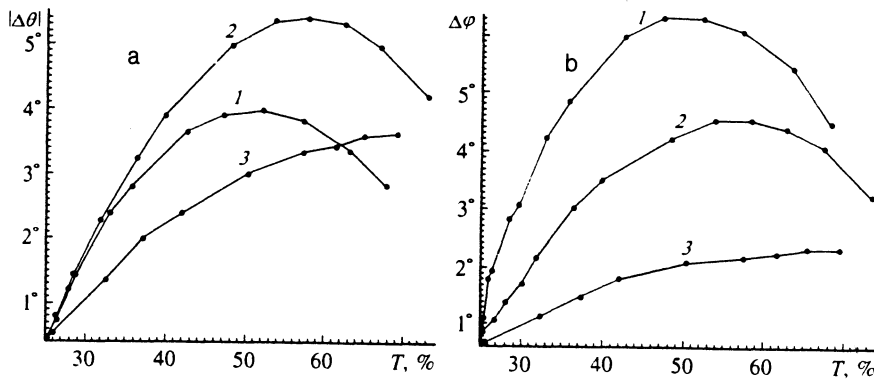


FIG. 8. Experimental curves of the angles  $|\Delta\theta|$  (a) and  $\Delta\varphi$  (b) as functions of the transmission coefficient  $T$  of a YAG:Cr<sup>4+</sup> crystal for certain values of the position  $\theta_0$  of the polarization plane of the wave at the entrance to the crystal:  $\theta_0=12.0^\circ$  (1),  $22.5^\circ$  (2), and  $33.0^\circ$  (3).

## 5. EXPERIMENTAL DETERMINATION OF THE PHASE RUNOUT IN YAG:Cr<sup>4+</sup> WITH ABSORPTION SATURATION

The possibility of investigating experimentally the nonlinear phase runout between the  $x$  and  $y$  components of a wave that interacts with a YAG:Cr<sup>4+</sup> crystal is certainly of interest. In this case the experiment is conducted under the same conditions as the measurement of the rotation of the polarization plane (see Sec. 3).

We now consider the energy  $E_2$  of the radiation passing through the polarizer–YAG:Cr<sup>4+</sup> crystal–analyzer system as a function of the angle  $\beta_0$ . With that system it is possible to measure not only the rotation angle  $\Delta\theta$  of the polarization plane but also the average phase difference  $\Delta\varphi$  arising between the  $x$  and  $y$  components of the electric vector during the pulse. Once the minimum  $\beta_0$  of the function  $E_2(\beta)$  [see Eq. (A9)] and thereby  $\Delta\theta$  have been determined, it is possible to estimate the phase difference  $\Delta\varphi$  arising with the passage through the crystal [see Eq. (A10)].

Figure 6b displays, in particular, the results of measurements of  $\Delta\varphi$  as a function of  $\theta_0$  performed by this method. The measurements were performed with average transmission of the crystal  $T \approx 60\%$ .

It was found that the best agreement between the experimental results and the theoretical calculations is obtained with  $\delta \approx 0.2$ . This demonstrates the possibility of estimating, in experiments of this type, the ratio of the imaginary and real parts of the susceptibility of a doped crystal with quiresonant excitation.

Figure 8 displays the angles  $\Delta\theta$  and  $\Delta\varphi$  as functions of the transmission  $T$ . The angles were measured for certain positions  $\theta_0$  of the polarization plane at the entrance to the YAG:Cr<sup>4+</sup> crystal. We call attention to the fact that, as follows from Fig. 8, the larger the angle  $\theta_0$ , the higher the transmission  $T$  of the crystal at the maxima of  $\Delta\theta(T)$  and  $\Delta\varphi(T)$ .

The data in Figs. 6 and 8 demonstrate the possibility of estimating simply the nonlinear phase mismatch that arises between the  $x$  and  $y$  components of a wave (and which is very small in absolute magnitude) in a doped cubic crystal at the absorption saturation stage.

## 6. CONCLUSIONS

Our experimental and theoretical investigation of the interaction of a short light pulse ( $\lambda \sim 1.06 \mu\text{m}$ ) with a YAG:Cr<sup>4+</sup> crystal showed the following:

1) Absorption saturation in YAG:Cr<sup>4+</sup> is accompanied by the onset of anisotropy of the transmission coefficient. The maximum transmission contrast is  $D \approx 30\%$ .

2) The transmission coefficient anisotropy induced by intense radiation propagating in YAG:Cr<sup>4+</sup> is accompanied by a self-induced change in the polarization state of the radiation. This is characterized by a) the phase mismatch  $\Delta\varphi$  between the  $x$  and  $y$  components of the wave (the wave is converted into an elliptically polarized wave) and b) the rotation of the major axis of the polarization ellipse by an angle  $\Delta\theta$ . In YAG:Cr<sup>4+</sup>, both  $\Delta\theta$  and  $\Delta\varphi$  reach  $\approx 5^\circ$  in absolute magnitude.

3) The proposed phenomenological description of the interaction of a short ( $\tau_p \ll T_{(2)}$ ) light pulse with a YAG:Cr<sup>4+</sup> crystal near a resonant transition is completely consistent with the experimental data. The quantitative agreement between the theoretical and experimental results indicates that the phototropic impurity centers are faithfully described by the theoretical model of three linear dipoles and, conversely, that significant discrepancies arise when such centers are considered to be Cr ions with valence 4 in a YAG lattice and thus described by a model of three circular dipoles.

4) The angular dependences  $T(\theta_0)$  and  $\Delta\theta(\theta_0)$  (Figs. 4 and 6) as well as the transmission contrast  $D$ , the maximum rotation angle  $\Delta\theta_{\text{max}}$  of the major axis of the polarization ellipse, and the width  $\Psi$  of the maximum as a function of the average transmission coefficient  $\bar{T}$  at the absorption saturation stage (Figs. 5 and 7) yield information about the properties of an impurity crystal, including general information about the distribution of impurities in the lattice, the type of interaction, the characteristics of the impurities, the presence of absorption from the excited state, and so on.

We wish to thank L. M. Ershov for determining the orientations of the crystallographic axes of the YAG:Cr<sup>4+</sup> crystal.

Financial support for this work was provided by the

**APPENDIX**

In experiments on determining the self-induced rotation  $\Delta\theta$  of the polarization plane and the runout  $\Delta\varphi$  in the phase difference between the  $x$  and  $y$  components of a wave propagating in an impurity crystal, the transmission function of the polarizer-crystal-analyzer system (see Fig. 1) is measured when the polarizer and analyzer are in a nearly crossed state. We describe below the measurement procedure in these experiments.

In accordance with Fig. 2, the components of the electric field vector of the wave at the entrance to the crystal are

$$\mathcal{E}^0 = \mathcal{E}^0 \begin{vmatrix} \sin \theta_0 \\ \cos \theta_0 \end{vmatrix}, \quad (A1)$$

and at the exit from the crystal

$$\mathcal{E}^L = \mathcal{E}^L \begin{vmatrix} e^{i\varphi_x} \sin(\theta_0 + \Delta\theta(t)) \\ e^{i\varphi_y} \cos(\theta_0 + \Delta\theta(t)) \end{vmatrix}, \quad (A2)$$

where  $\mathcal{E}^L = \sqrt{T}E^0$ .

The direction of the unit vector  $\mathbf{n}_\beta$  that corresponds to minimum transmission of the analyzer is given by

$$\mathbf{n}_\beta = \begin{vmatrix} \cos(\theta_0 + \beta) \\ -\sin(\theta_0 + \beta) \end{vmatrix}. \quad (A3)$$

The energy  $E_2$  of a pulse passing through the polarizer-crystal-analyzer system is determined by the relation

$$E_2(\beta) \propto \int_{-\infty}^{\infty} I_\beta(t) dt \propto \int_{-\infty}^{\infty} (\mathcal{E}^L(t), \mathbf{n}_\beta)^2 dt. \quad (A4)$$

Using Eqs. (A2) and (A3), we obtain for the intensity  $I_\beta(t)$  measured in the  $\mathbf{n}_\beta$  direction

$$I_\beta(t) = I(t) \left\{ \cos^2 \frac{\Delta\varphi(t)}{2} \sin^2(\Delta\theta(t) - \beta) + \sin^2 \frac{\Delta\varphi(t)}{2} \sin^2(2\theta_0 + \Delta\theta(t) + \beta) \right\}. \quad (A5)$$

Next we assume that  $\beta$ ,  $\Delta\theta(t)$  and  $\Delta\varphi(t) \ll 1$  (which corresponds to the experimental data). Expanding the function in Eq. (A5) in a Taylor series and retaining terms up to  $[\Delta\theta(t)]^2$  and  $[\Delta\varphi(t)]^2$ , we obtain for the energy  $E_2(\beta)$

$$E_2(\beta) = A'\beta^2 + B'\beta + C', \quad (A6)$$

where the expansion coefficients are

$$\begin{aligned} A' &= 1 - 2\overline{(\Delta\theta)^2} - \frac{1}{4}\overline{(\Delta\varphi)^2}, \\ B' &= -2\Delta\theta + \frac{1}{4}\overline{(\Delta\varphi)^2}, \\ C' &= \overline{(\Delta\theta)^2} + \frac{1}{8}\overline{(\Delta\varphi)^2}, \end{aligned} \quad (A7)$$

and

$$\overline{(\Delta\theta)^2} = \frac{\int_{-\infty}^{\infty} I(\Delta\theta)^2 dt}{\int_{-\infty}^{\infty} I dt}, \quad \overline{(\Delta\varphi)^2} = \frac{\int_{-\infty}^{\infty} I(\Delta\varphi)^2 dt}{\int_{-\infty}^{\infty} I dt}, \quad (A8)$$

and  $\Delta$  is determined by (14).

Neglecting the quadratic terms in the expansion in Eq. (A7), we obtain for the position of the transmission minimum of the system

$$\beta_0 \equiv \beta|_{\partial E_2(\beta)/\partial \beta = 0} = -\frac{B'}{2A'} \approx \Delta\theta. \quad (A9)$$

In measuring the self-induced rotation of the polarization plane of the radiation, the average rotation  $\Delta\theta$  is measured in accordance with Eq. (A9). This approximation corresponds best to the purely resonant case ( $\Delta\varphi=0$ ) of the interaction of a light pulse with the medium.

There can arise the question of how legitimate such a measurement is for radiation at  $\lambda \sim 1.06 \mu\text{m}$  interacting with a YAG:Cr<sup>4+</sup> crystal. Here it is the magnitude of the difference of the phase increments between the  $x$  and  $y$  components of the wave due to the detuning of the radiation from exact resonance of the transition that is actually of concern.

Since the angles  $\beta$ ,  $\Delta\theta(t)$ , and  $\Delta\varphi(t)$  are small, even in this case Eq. (A9) can be used to calculate, to a good degree of accuracy, the average rotation angle  $\Delta\theta$  of the polarization. In other words, the contribution of the difference of the phase increments to the value of  $\Delta\theta$  measured by the indicated method is small.

The quantity  $\Delta\varphi$ , however, must be determined by starting with the second or third expression in Eq. (A7), using now the measured value of  $\Delta\theta$ . Setting  $(\Delta\theta)^2 = \overline{(\Delta\theta)^2}$ , the average value of the difference  $\Delta\varphi$  between the phase increments is

$$\Delta\varphi \approx \frac{2}{\sin 2\theta_0} \sqrt{C' - (\Delta\theta)^2}. \quad (A10)$$

In conclusion, it should be noted that the experimental accuracy with which  $\Delta\varphi$  can be determined from Eq. (A10) should decrease as  $\theta_0$  approaches the values  $0^\circ$ ,  $\pm 90^\circ, \dots$

<sup>1</sup>V. M. Garmash, N. I. Borodin, L. A. Ermakova *et al.*, *Elektron. Tekhnika*, Ser. 11 (Lasernaya tekhnika i optoelektronika) **3**, 20 (1989).

<sup>2</sup>D. T. Sviridov and S. D. Sviridova, *Zh. Prikl. Spektrosk.* **49**, 146 (1988).

<sup>3</sup>A. G. Okhrimchuk, A. V. Shestakov, and V. A. Zhitnyuk, *Elektron. Tekhnika*, Ser. 11 (Lasernaya tekhnika i optoelektronika) **2**, 20 (1990).

<sup>4</sup>L. I. Krutova, A. V. Lunin, V. A. Sandulenko *et al.*, *Opt. Spektrosk.* **63**, 1174 (1987) [*Opt. Spectrosc.* **63**, 693 (1987)].

<sup>5</sup>L. I. Krutova, N. A. Kulagin, V. A. Sandulenko *et al.*, *Fiz. Tverd. Tela* **31**, 170 (1989) [*Sov. Phys. Solid State* **31**, 1193 (1989)].

<sup>6</sup>V. M. Garmash, V. A. Zhitnyuk, A. G. Okhrimchuk *et al.*, *Izv. Akad. Nauk SSSR, Neorg. Mater.* **26**, 1700 (1990).

<sup>7</sup>M. I. Demchuk, N. V. Kuleshov, V. P. Mikhailov *et al.*, *Zh. Prikl. Spektrosk.* **51**, 337 (1989).

<sup>8</sup>V. N. Sazonov, *Chromium in the Hydrothermal Process* [in Russian], Moscow (1978), p. 287.

<sup>9</sup>V. Petricevic, S. K. Gayen, and R. R. Alfano, *Appl. Phys. Lett.* **53**, 2590 (1988).

<sup>10</sup>M. I. Demchuk, E. V. Zhrikov, A. M. Zabaznov *et al.*, *Kvant. Elektron.* **14**, 423 (1987) [*Sov. J. Quantum Electron.* **17**, 266 (1987)].

- <sup>11</sup>D. M. Andrauskas and C. Kennedy, in *Proceedings on Advanced Solid-State Lasers*, G. Dube and L. Chase (eds.), Optical Society of America, Washington (1991), Vol. 10, p. 393.
- <sup>12</sup>E. V. Zhrikov, A. M. Zabaznov, A. M. Prokhorov *et al.*, *Kvant. Elektron.* **13**, 2347 (1986) [*Sov. J. Quantum Electron.* **16**, 1552 (1986)].
- <sup>13</sup>A. G. Okhrimchuk, *Spectroscopic, luminescence, and lasing properties of Cr<sup>4+</sup>-activated yttrium-aluminum garnet crystals*, *Candidate's Dissertation in Physicomathematical Sciences*, IOFAN, Moscow (1991).
- <sup>14</sup>N. I. Borodin, V. A. Zhitnyuk, A. G. Okhrimchuk *et al.*, *Izv. Akad. Nauk SSSR, Ser. Fiz.* **54**, 1500 (1990).
- <sup>15</sup>N. B. Angert, N. I. Borodin, V. M. Garmash *et al.*, *Kvant. Elektron.* **15**, 113 (1988) [*Sov. J. Quantum Electron.* **18**, 73 (1988)].
- <sup>16</sup>N. N. Il'ichev, A. V. Kir'yanov, A. A. Malyutin *et al.*, *Laser Phys.* **3**, 182 (1993).
- <sup>17</sup>N. N. Il'ichev, A. V. Kir'yanov, and A. A. Malyutin, *Laser Phys.* **1**, 311 (1991).
- <sup>18</sup>H. Eilers, K. R. Hoffman, W. M. Dennis *et al.*, *Appl. Phys. Lett.* **61**, 2958 (1992).
- <sup>19</sup>N. N. Il'ichev, A. A. Malyutin, P. P. Pashinin *et al.*, *Kvant. Elektron.* **19**, 589 (1992) [*Sov. J. Quantum Electron.* **22**, 543 (1992)].
- <sup>20</sup>P. A. Apanasevich and V. G. Dubovets, *Zh. Prikl. Spektrosk.* **17**, 796 (1972).
- <sup>21</sup>M. I. Dykman and G. G. Tarasov, *Zh. Eksp. Teor. Fiz.* **72**, 2246 (1977) [*Sov. Phys. JETP* **45**, 1181 (1977)].
- <sup>22</sup>S. A. Mikhnov, V. S. Kalinov, S. I. Ovseichuk *et al.*, in *Proceedings of the Fifth International Conference on Tunable Lasers, September 20-22, 1989, Baikal, SSSR, Novosibirsk* (1990), Part 1, p. 163.
- <sup>23</sup>A. A. Mak, V. P. Pokrovskii, V. P. Soms *et al.*, *Kvant. Elektron.* **9**, 1607 (1982) [*Sov. J. Quantum Electron.* **9**, 1030 (1982)].

Translated by M. E. Alferieff